Mesospheric Precursors to the Major Stratospheric Sudden Warming of 2009: Validation and Dynamical Attribution using a Ground-to-Edge-of-Space Data Assimilation System

L. Coy [1]*, S. D. Eckermann* [1]*, K. W. Hoppel* [2]*, and F. Sassi* [1]

[1]Space Science Division, Naval Research Laboratory, Code 7646, 4555 Overlook Avenue, SW, Washington, DC 20375-5320, USA.
[2]Remote Sensing Division, Naval Research Laboratory, Code 7227, 4555 Overlook Avenue, SW, Washington, DC 20375-5320, USA.

Global meteorological analyses from an assimilation of operational and research observations spanning the $\sim$0-90 km altitude range confirm earlier tentative suggestions that high-altitude winds throughout the upper mesosphere reversed a week before the major stratospheric sudden warming (SSW) of January 2009. Analyzed winds reveal descent of mean easterlies from the upper mesosphere to the lower stratosphere, followed by more easterly winds throughout the Arctic troposphere in the weeks after the SSW, indicating that these descending Northern Annular Mode (NAM) anomalies reached the surface. Eliassen-Palm fluxes reveal that the mesospheric precursor to this event was driven by transient nonstationary wave-2 planetary waves that propagated rapidly from the troposphere into the upper mesosphere, where they dissipated and produced easterly mean-flow accelerations. This early SSW phase was characterized by both descending mesospheric easterlies and poleward expansion of subtropical stratospheric easterlies, which eventually merged in the extratropical upper stratosphere. These wind structures may in turn have focused transient wave-2 PW activity emerging from the troposphere in ways that intensified the SSW.

1. Introduction

Early modeling and observations inferred deep cooling of the winter polar mesosphere during stratospheric sudden warmings (SSWs) (Matsuno, 1971; Labitzke, 1981; Holton, 1983). Only recently have satellite temperature observations expanded this view by revealing richer and more variable mesospheric thermal responses to SSWs. Typically, mesospheric cooling layers are shallow and give way to a warming response in the lower thermosphere (e.g. Siskind et al., 2005). During the major SSW of January 2006, however, the winter polar stratopause disappeared, then reformed in the upper mesosphere and slowly descended over a period of weeks (Manney et al., 2008). Since wind observations are sparse and standard data assimilation systems (DASs) do not extend through the mesosphere, we have far less observational informa-tion on dynamical responses of the mesosphere during SSWs.

The record-breaking wave-2 major SSW of January 2009 produced somewhat similar mesospheric thermal responses to the January 2006 wave-1 event (Manney et al., 2009). Gradient winds inferred from Microwave Limb Sounder (MLS) temperatures (Manney et al., 2009) and ground-based radar wind measurements from a high-latitude site (Kurihara et al., 2010) each suggested that winds reversed in the mesosphere about a week before the stratospheric wind reversal. Winds inferred from MLS also showed descent of zero wind lines from the upper mesosphere into the stratosphere, which Lee et al. (2009) interpreted as downward-propagating anomalies in the Northern Annular Mode (NAM) that formed first in the upper mesosphere.

Yet it remains unclear: (a) if, why and how meso-

Report Documentation Page

Form Approved
OMB No. 0704-0188

1. REPORT DATE **JAN 2011**	2. REPORT TYPE	3. DATES COVERED **00-00-2011 to 00-00-2011**

4. TITLE AND SUBTITLE **Mesospheric Precursors to the Major Stratospheric Sudden Warming of 2009: Validation and Dynamical Attribution using a Ground-to-Edge-of-Space Data Assimilation System**	5a. CONTRACT NUMBER
	5b. GRANT NUMBER
	5c. PROGRAM ELEMENT NUMBER
6. AUTHOR(S)	5d. PROJECT NUMBER
	5e. TASK NUMBER
	5f. WORK UNIT NUMBER

7. PERFORMING ORGANIZATION NAME(S) AND ADDRESS(ES) **Naval Research Laboratory,Space Science Division, Code 7646,4555 Overlook Avenue, SW,Washington,DC,20375-5320**	8. PERFORMING ORGANIZATION REPORT NUMBER

9. SPONSORING/MONITORING AGENCY NAME(S) AND ADDRESS(ES)	10. SPONSOR/MONITOR'S ACRONYM(S)
	11. SPONSOR/MONITOR'S REPORT NUMBER(S)

12. DISTRIBUTION/AVAILABILITY STATEMENT
Approved for public release; distribution unlimited

13. SUPPLEMENTARY NOTES

14. ABSTRACT

15. SUBJECT TERMS

16. SECURITY CLASSIFICATION OF:			17. LIMITATION OF ABSTRACT	18. NUMBER OF PAGES	19a. NAME OF RESPONSIBLE PERSON
a. REPORT **unclassified**	b. ABSTRACT **unclassified**	c. THIS PAGE **unclassified**	**Same as Report (SAR)**	**8**	

Standard Form 298 (Rev. 8-98)
Prescribed by ANSI Std Z39-18

spheric winds reversed throughout the polar region a week before similar reversals occurred throughout the polar stratosphere, and (b) whether the inferred subsequent descent of these initial mesospheric NAM anomalies into the stratosphere played a significant role in the timing and strength of the 2009 SSW. We address these questions here by studying the dynamics of the 2009 SSW from ∼0-100 km altitude using global meteorological analyses from a DAS that assimilated satellite temperatures through the stratosphere and mesosphere.

2. DAS Fields and Diagnostics

We use 6-hourly global meteorological analyses from an Advanced Level Physics High-Altitude (ALPHA) prototype of the Navy Operational Global Atmospheric Prediction System (NOGAPS). The DAS fields were generated using the production NOGAPS-ALPHA configuration described by Eckermann et al. (2009). Briefly, the forecast model ran at T79 (∼2.25° latitude-longitude resolution) with 68 model levels extending from the ground to ∼0.0005 hPa, and interfaced to the Naval Research Laboratory three-dimensional variational DAS (NAVDAS: Daley and Barker 2001) in a fully-coupled 6-hourly forecast-assimilation update cycle. In addition to archived operational sensor data from lower altitudes, the system assimilated limb temperatures from the MLS and SABER (Sounding of the Atmosphere using Broadband Emission Radiometry) instruments on NASA's Aura and TIMED research satellites, respectively, up to 0.002 hPa (∼90 km), well above the altitudes spanned by the operational sensor data.

In computing Eliassen-Palm (EP) fluxes $\mathbf{F} = (F^\phi, F^z)$ from these fields, we ignore the vertical momentum flux term, $\overline{w'u'}$, which is small for the planetary-wave (PW) motions studied here. To display small mesospheric EP fluxes, we normalize fluxes at each analysis level by their maximum amplitude between 1 December 2008 and 28 February 2009. All quantities plotted here are daily averages.

3. Results

Figure 1 plots time series of analyzed zonal-mean quantities at high latitudes from 0-100 km altitude during the 2009 northern winter.

Polar temperatures (Fig. 1a) show that the major SSW on 24 January was accompanied first by upper mesospheric cooling, then by disappearance of the

stratopause near 1 hPa and reformation at ∼0.01 hPa in February. These features agree well with the MLS temperatures presented by Manney et al. (2009). The analyzed zonal winds at 60°N (Fig. 1b) show zero wind lines appearing first in the upper mesosphere, then descending to 10 hPa about a week later, in agreement with gradient winds derived diagnostically from MLS temperatures (Manney et al., 2009). Analyzed winds throughout the troposphere are persistently weaker in the weeks after the SSW relative to those before it. Zonal winds at 75°N (Fig. 1e) reveal progressive descent of easterlies from the upper mesosphere to the surface.

To validate our analyzed mesospheric wind responses, Fig. 2 compares time series of diurnally averaged zonal winds at 80 km measured by the NTMR (Nippon/Norway Tromsø Meteor Radar) at 69.9°N, 19.2°E (Kurihara et al., 2010) with DAS winds at the same height and location. There is excellent agreement between the two time series. Specifically, NTMR winds validate the analyzed reversal of mesospheric winds by 17 January and the persistence of mean easterlies until 29 January.

Panels (c) and (d) of Fig. 1 show meridional wind amplitude at 60°N of wavenumber 1 (Fig. 1c) and wavenumber 2 (Fig. 1d) PW disturbances. Wave-2 PW amplitudes peak in excess of 90 m s^{-1} during the SSW, consistent with 2009 being a wave-2 (split vortex) SSW (Harada et al., 2010). Both wave-1 and wave-2 amplitudes are much weaker after the SSW, though there is evidence of a high-altitude wave-1 PW forming after the SSW, as also occurred in 2006 (Manney et al., 2008).

Figure 1f plots a time-height cross section of wave-2 F^z at 60°N, scaled by $\exp(z/2H)$, where z is pressure altitude and H =7 km. As in Harada et al. (2010), largest 100 hPa values occur on 19 January after a buildup of flux beginning ∼10 January. During this buildup phase, EP fluxes extend into the upper mesosphere at the same time that winds here reverse to easterlies. Vertical PW propagation from the troposphere to the upper mesosphere is rapid at this time (∼1–3 days), in contrast to three earlier wave-2 events in December that propagated more slowly and are confined to the stratosphere. After the SSW (24 January), two additional rapid pulses of wave-2 flux extend above the 1 hPa level and through descending easterlies.

Longitude-height cross sections of geopotential height perturbations (GHPs) at 60°N in Fig. 3 also show rapid wave-2 PW propagation into the upper mesosphere. On 12 January (Fig. 3a), GHPs are weak and disorga-
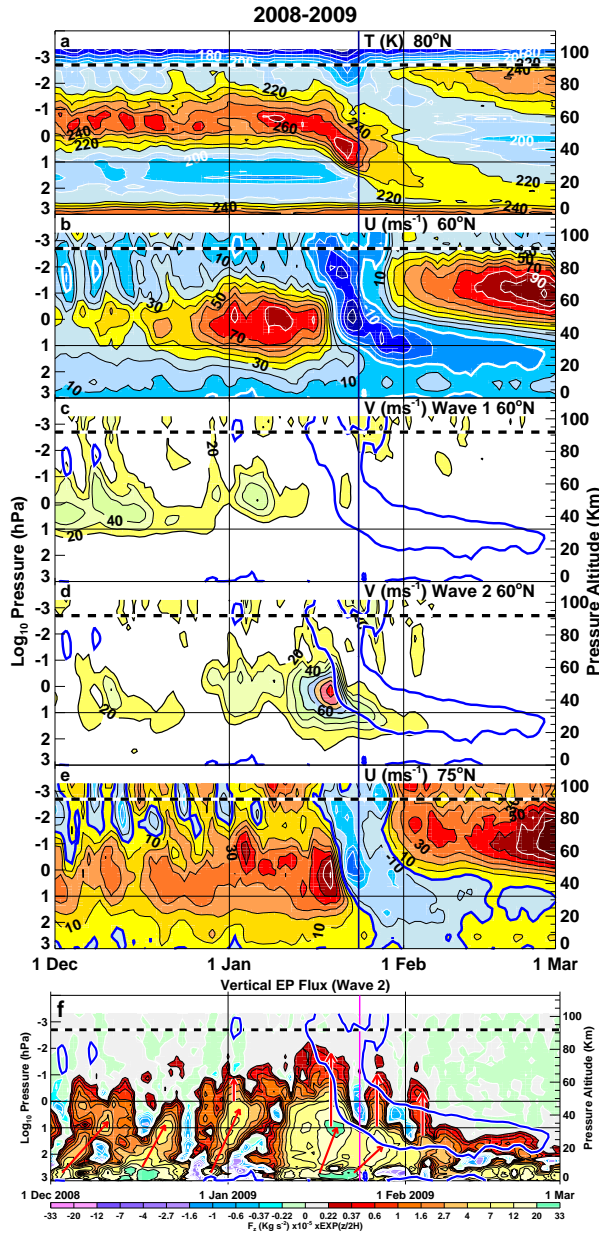
Figure 1: Time series from 0-100 km of (a) zonal-mean temperature (K) at 80°N; (b) zonal-mean zonal wind (m s^{-1}) at 60°N; (c) wave-1 and (d) wave-2 meridional wind amplitude (m s^{-1}) at 60°N; (e) zonal-mean zonal wind (m s^{-1}) at 75°N, and; (f) $F^z \exp(z/2H)$ for wavenumber 2 at 60°N. Heavy white contour in (b) and blue contours in (c) (d) and (f) show zero zonal wind lines at 60°N. Horizontal dashed line at 0.002 hPa marks top data ingestion level. Red arrows in (f) depict group velocity propagation of PW bursts.
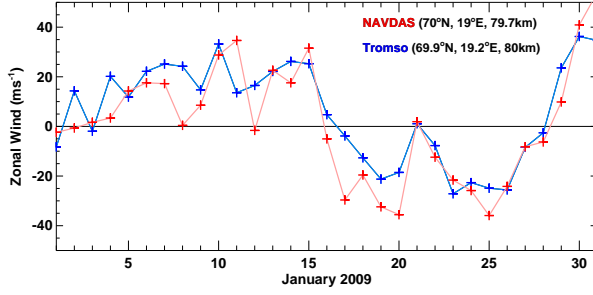
Figure 2: Daily averaged zonal winds at 80 km over Tromsø, Norway (69.9°N, 19.2°E) during January 2009 from NOGAPS-ALPHA DAS (red curve) and as measured by the NTMR (blue curve: after Kurihara et al., 2010).

nized. By 16 January (Fig. 3b), GHPs are larger and show a coherent westward-tilted wave-2 pattern that extends from the troposphere to the upper mesosphere, characteristic of an upward propagating PW. Even as upper mesospheric easterlies form and descend (18 January: Fig. 3c), westward-tilted GHPs continue to extend through the mesosphere. As easterlies finally descend into the stratosphere (20 January: Fig. 3d), the westward-tilted wave-2 GHPs only extend to the lower mesosphere.

Figure 4 plots EP flux vectors, EP flux divergence, and zonal-mean zonal winds on 12, 16, 18, and 20 January. EP fluxes show the expected upward and equatorward PW propagation, and extend deep into the mesosphere by 16 January (Fig. 4b) when zero zonal-wind lines (black-outlined white curves in Fig. 4b) appear in the upper mesosphere, well in advance of any zero zonal wind lines at 60°N in the stratosphere. These high-latitude upper mesospheric easterlies are distinct from the subtropical stratospheric easterlies also developing at this time. By 18 January (Fig. 4c), the two easterly regions in the tropical stratosphere and extratropical mesosphere remain separate, but have extended further poleward and downward, respectively. By 20 January (Fig. 4d), the two regions have joined to form a contiguous band of easterlies extending from the polar mesosphere to the tropical stratosphere.

In regions of Figure 4 where GHP amplitudes exceed 200 m, red solid curves show the PW critical line (CL): i.e., where wave-2 PW horizontal phase speed equals the zonal-mean zonal wind speed. On 12 January two CLs, one stratospheric and one mesospheric, are evident, each well separated from the zero wind lines at those altitudes, indicating nonzero PW phase speeds. By 16 January (Fig. 4b) the stratospheric CL has shifted equatorward and intersects the zero wind line

in the upper stratosphere, while the mesospheric CLs intersect a newly-formed high-altitude zero wind line. Two days later (18 January) the 40°N CL in the upper stratosphere extends well into the mesosphere and nearly merges with the high-altitude mesospheric CL. By 20 January (Fig. 4d) two CLs have formed, the lower one closely tracking the lower zero-wind line (suggesting quasi-stationary PWs), and the upper curve offset just below another zero wind-line, indicating weak westerly PW phase speeds (<20 m s^{-1}). Thus, wave-2 PW activity shows large variations in horizontal phase speed, especially during the early stages of the SSW. Transience induced as the stratosphere responds to vacillating tropospheric PW forcing is one likely cause of these variations.

Shaded contours in Figure 4 show mean-flow accelerations due to PW EP-flux divergence, $(\rho a \cos \phi)^{-1} \nabla \cdot \mathbf{F}$. PW dissipation begins in the mesosphere (Fig. 4a) and intensifies by 16 January (Fig. 4b), forcing easterly accelerations of 20–40 m s^{-1} day^{-1} over a deep region from the upper mesosphere to the stratopause. Such sustained accelerations appear sufficient to drive the observed upper mesospheric wind reversal at this time. Mesospheric PW forcing persists to 18 January (Fig. 4c), causing mesospheric easterlies to descend, and stronger PW accelerations now also occur near the stratopause, with subtropical stratospheric easterlies drawn poleward. By 20 January easterlies have descended into the upper stratosphere, mesospheric PW driving is now weaker and easterly PW forcing at the polar stratopause peaks in excess of 100 m s^{-1} day^{-1}.
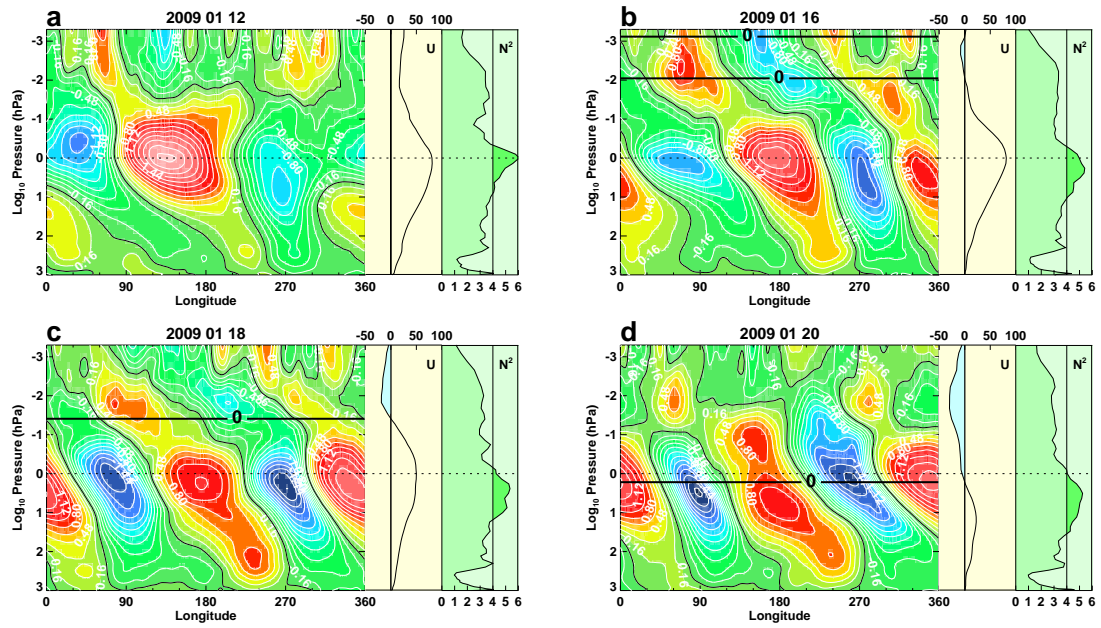
Figure 3: Longitude-height cross sections of 60°N GHPs (contour interval 0.16 km) on (a) 12, (b) 16, (c) 18, and (d) 20 January 2009. Zero contour is denoted by black curves. To the right of each panel are profiles of zonal-mean zonal wind (m s^{-1}) and stability (10^{-4}s^{-2}) at 60°N.
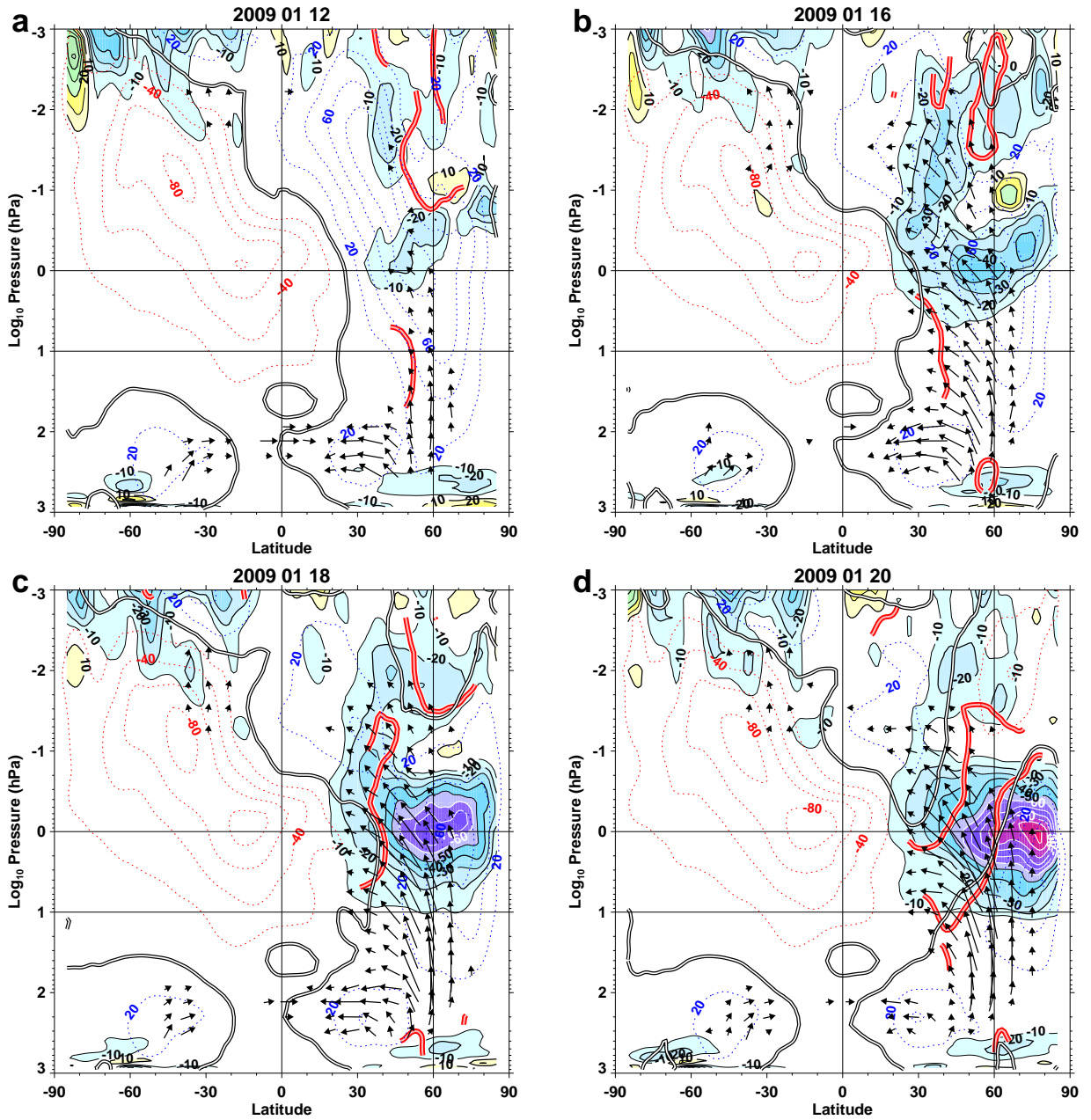
Figure 4: Latitude-height cross sections of EP flux **F** (arrows), $(\rho a \cos \phi)^{-1} \nabla \cdot \mathbf{F}$ (color-shaded contours, contour interval 10 m s^{-1} day^{-1}), and zonal-mean zonal winds (dotted, contour interval 20 m s^{-1}), for (a) 12, (b) 16, (c) 18, and (d) 20 January 2009. Zero zonal-wind line is plotted with black-outlined white contour. Red-outlined curves (shown only where GHP amplitude >200 m) show wave-2 critical lines.

4. Summary

We have used a prototype high-altitude DAS to assimilate observations from the ground to the edge of space ($\sim$0–90 km) during the northern winter of 2009. Our study of the global meteorological analysis fields that were produced by this system revealed that wind reversals at high northern latitudes in January 2009 occurred first in the upper mesosphere, about a week prior to the 10 hPa 60°N wind reversal that defined the 2009 SSW as "major." These fields furthermore revealed that this mesospheric precursor to the SSW was driven by transient wave-2 PW activity that propagated rapidly from the troposphere into the upper mesosphere, where it dissipated, yielding persistent easterly accelerations of 20–40 m s^{-1} day^{-1} that led to rapid descent of easterly mesospheric shear zones.

Analyzed winds (Figs. 1b and 1e) show coherent descent with time of easterlies from the upper mesosphere to the lower stratosphere, which Lee et al. (2009) interpreted as downward-propagating NAM anomalies initiated in the upper mesosphere. Indeed, Figures 1b and 1e show that these easterly wind anomalies eventually reached the surface, with tropospheric winds becoming systematically more easterly for several weeks after the SSW relative to those before it, consistent with modified Arctic weather due to these downward-propagating NAM anomalies (Baldwin and Dunkerton, 2001).

However, our DAS fields showed that easterlies did not simply form in the extratropical upper mesosphere and propagate downward. Rather, descending extratropical mesospheric easterlies merged with a poleward march of subtropical stratospheric easterlies. Thus, the importance of mesospheric easterlies to the initiation and ultimate strength of the 2009 SSW is difficult to quantify, since PWs tend to propagate into subtropical stratospheric easterlies irrespective of the upper mesospheric wind profile. Furthermore, the wave-2 PWs driving this event exhibited variable nonstationary phase speeds as they propagated into the stratosphere. In the early stages, stratospheric CLs occurred well north of the subtropical zero wind line, which may have focused PWs towards more vertical propagation, thereby increasing their amplitudes in the extratropical mesosphere. At later times, we observed large-amplitude PW activity crossing stratospheric CLs, but these anomalous propagation events abated by late January as easterlies descended into the lower stratosphere.

References

Baldwin, M. P., and T. J. Dunkerton, 2001: Stratospheric harbingers of anomalous weather regimes, *Science*, 294, 581–584.

Daley, R., and E. Barker, 2001: NAVDAS: Formulation and diagnostics, *Mon. Wea. Rev.*, 129, 869–883.

Eckermann, S. D., K. W. Hoppel, L. Coy, J. P. McCormack, D. E. Siskind, K. Nielsen, A. Kochenash, M. H. Stevens, C. R. Englert, W. Singer, and M. Hervig, 2009: High-altitude data assimilation system experiments for the northern summer mesosphere season of 2007, *J. Atmos. Sol.-Terr. Phys.*, 71, 531–551.

Harada, Y., G. Atsushi, H. Hiroshi, and N. Fujikawa, 2010: A major stratospheric sudden warming event in January 2009, *J. Atmos. Sci.*, 67, 2052–2069.

Holton, J. R., 1983: The influence of gravity wave breaking on the general circulation of the middle atmosphere, *J. Atmos. Sci.*, 40, 2497–2507.

Kurihara, J., Y. Ogawa, S. Oyama, S. Nozawa, M. Tsutsumi, C. M. Hall, Y. Tomikawa, and R. Fujii, 2010: Links between a stratospheric sudden warming and thermal structures and dynamics in the high-latitude mesosphere, lower thermosphere, and ionosphere, *Geophys. Res. Lett.*, 37, L13806, doi:10.1029/2010GL043643.

Labitzke, K., 1981: Stratospheric-mesospheric midwinter disturbances: A summary of observed characteristics, *J. Geophys. Res.*, 86, 9665–9678.

Lee, J. N., D. L. Wu, G. L. Manney, and M. J. Schwartz, 2009: Aura Microwave Limb Sounder observations of the Northern Annular Mode: From the mesosphere to the upper troposphere, *Geophys. Res. Lett.*, 36, L20807, doi:10.1029/2009GL040678.

Manney, G. L., et al., 2008: The evolution of the stratopause during the 2006 major warming: Satellite data and assimilated meteorological analyses, *J. Geophys. Res.*, 113, D11115, doi:10.1029/2007JD009097.

Manney, G. L., M. J. Schwartz, K. Krüger, M. L. Santee, S. Pawson, J. N. Lee, W. H. Daffer, R. A. Fuller, and N. J. Livesey, 2009: Aura Microwave Limb Sounder observations of dynamics and transport during the record-breaking 2009 Arctic stratospheric major warming, *Geophys. Res. Lett.*, 36, L12815, doi:10.1029/2009GL038586.

Matsuno, T., 1971: A dynamical model of the stratospheric sudden warming, *J. Atmos. Sci.*, 28, 1479–1494.

Siskind, D. E., L. Coy, and P. Espy, 2005: Observations of stratospheric warmings and mesospheric coolings by the TIMED SABER instrument, *Geophys. Res. Lett.*, 32, L09804, doi:10.1029/2005GL022399.